Received: 4 November 2021 | Revised: 23 March 2022 | Accepted: 12 April 2022

DOI: 10.1111/joa.13681

Journal of Anatomy ANATOMICAL SOCIETY WILEY

BRIEF COMMUNICATION

Exploring the relationship between soft and hard tissues: The example of vertebral arteries and transverse foramina

Edwin de Jager[1] | Lané Prigge[2,3] | Nooreen Amod[4] | Anna Oettlé[2,3] | Amélie Beaudet[1,5,6]

[1]Department of Archaeology, University of Cambridge, Cambridge, UK

[2]Department of Anatomy, Sefako Makgatho Health Sciences University, Ga-Rankuwa, South Africa

[3]Department of Anatomy, University of Pretoria, Pretoria, South Africa

[4]Department of Radiology, Dr George Mukhari Academic Hospital, Ga-Rankuwa, South Africa

[5]School of Geography, Archaeology and Environmental Studies, University of the Witwatersrand, Johannesburg, South Africa

[6]Institut Català de Paleontologia Miquel Crusafont, Universitat Autònoma de Barcelona, Barcelona, Spain

Correspondence
Amélie Beaudet, Department of Archaeology, University of Cambridge, Cambridge, UK.
Email: aab88@cam.ac.uk

Funding information
Erasmus plus programme, Grant/Award Number: 597924-EPP-1-2018-1-ZA-EPPKA2-CBHE-JP 2018-3229; National Research Foundation of South Africa, Grant/Award Number: 129336; South Africa/France (PROTEA) Joint Research Programme, Grant/Award Number: 129923; National Research Foundation, Grant/Award Number: EPPKA2-CBHE-JP

Abstract

Understanding how the brain is provided with glucose and oxygen is of particular interest in human evolutionary studies. In addition to the internal carotid arteries, vertebral arteries contribute significantly to the cerebral and cerebellar blood flow. The size of the transverse foramina has been suggested to represent a reliable proxy for assessing the size of the vertebral arteries in fossil specimens. To test this assumption, here, we statistically explore spatial relationships between the transverse foramina and the vertebral arteries in extant humans. Contrast computed tomography (CT) scans of the cervical regions of 16 living humans were collected. Cross-sectional areas of the right and left transverse foramina and the corresponding vertebral arteries were measured on each cervical vertebra from C1 to C6 within the same individuals. The cross-sectional areas of the foramina and corresponding arteries range between 13.40 and 71.25 mm^2 and between 4.53 and 29.40 mm^2, respectively. The two variables are significantly correlated except in C1. Using regression analyses, we generate equations that can be subsequently used to estimate the size of the vertebral arteries in fossil specimens. By providing additional evidence of intra- and inter-individual size variation of the arteries and corresponding foramina in extant humans, our study introduces an essential database for a better understanding of the evolutionary story of soft tissues in the fossil record.

KEYWORDS
blood flow, brain perfusion, cervical vertebrae, CT scans, metabolism

1 | INTRODUCTION

Even though the extant human brain only accounts for 2.5% of the body's weight, it receives one-sixth of the cardiac output and requires 20%–25% of the basal metabolic rate (Hublin et al., 2015; Moore et al., 2018). Because of the central role of the brain in the emergence of modern human biology and behavior, the question of how to "feed" an evolving brain and how the vascular and metabolic system of the hominin brain changed through time, are of particular interest (Lieberman, 2011). Unfortunately, since soft tissues

do not fossilize, reconstructing cerebral blood flow in extinct species is particularly challenging and, consequently, data documenting fossil hominin brain perfusion, and metabolism are particularly scarce (Leonard & Robertson, 1994; Leonard et al., 2003; Seymour et al., 2016).

In their landmark study, Seymour et al. (2016) estimated cerebral blood flow rate from the size of the carotid canals in fossil hominin basicrania and suggested a recent emergence of the human-like metabolic pattern in the hominin lineage. However, a subsequent study revealed that the vertebral arteries in extant euarchontans (including hominoids) contribute significantly to cerebral and cerebellar blood flow and that the total encephalic arterial canal area (i.e, not only the carotid canals but also the transverse foramina of the cervical vertebrae) is the most reliable proxy for estimating brain perfusion and metabolism (Boyer & Harrington, 2018).

The vertebral artery arises from the first part of the subclavian artery and ascends between the longus coli and anterior scalene muscles in order to pass through the transverse foramen of the sixth cervical vertebra. It continues to ascend through the consecutive cervical vertebrae until it reaches the first cervical vertebra, after which it curves medially around the lateral mass of the atlas. It finally enters the cranium via the foramen magnum and forms part of the vertebrobasilar arterial system of the brain (Standring et al., 2008). As such, the cervical vertebrae represent a key element in the cerebral vascular system due to the vertebral arteries ascending through the transverse foramina and providing the brain with arterial blood.

Given the rising interest in the study of vertebral arteries in fossil hominins (e.g., Beaudet et al., 2020), in this study, we statistically explore spatial relationships between the transverse foramina and the vertebral arteries in the cervical segment of the human vertebral column. More specifically, this study aims to (i) measure the cross-sectional areas of the transverse foramina and the vertebral arteries passing through the cervical vertebrae from C1 to C6 and (ii) to statistically investigate correlations that could be subsequently used to predict the size of the vertebral arteries in fossil hominins.

2 | MATERIALS AND METHODS

2.1 | Sample

Computer tomography (CT) scans of the cervical segment of the vertebral column of living human individuals were collected from the Department of Radiology at an academic referral hospital in the Gauteng province (South Africa; following ethical guidance provided by the hospital, the name of this institution should remain confidential). These CT scan images are utilized for clinical diagnosis for indications that include trauma, evaluation of aneurysms, blood clots, arteriovenous malformations, masses, and its effects on the adjacent structure. Post-contrast computed tomography scans of the neck were collected after ethical clearance was obtained from the related tertiary university and approval was granted by the specific hospital's superintendent. Individuals with pathologies or trauma were systematically excluded from the study. The sample of this pilot study comprises at the moment 16 individuals (including 5 females and 11 males) with an age ranging from 21 to 75 years, all from South Africa.

2.2 | Scanning procedure

The CT neck protocol at this hospital includes a scout view, pre-contrast and post-contrast study of a patient placed in the supine position within the gantry. Images were collected using a Phillips 128 Ingenuity CT scanner and the GE Optima 660,128 Slice CT scanner. The contrasting portion of the study includes the injection of contrast medium into the blood vessels. Injection of 50–75 ml of iodinated contrast with a pump injector at a rate of 3 ml/s ensures minimal scan delay. The radiographers capture high-resolution CT images while the contrast medium flows through the blood vessels. Scans are timed to ensure maximal opacification and decrease venous contamination.

The scan length starts from the base of the skull to the aortic arch in a cranio-caudal direction with a slice thickness ranging from 0.5 to 1 mm. A 32 cm collimation is used to limit the beam and thus reduce unnecessary radiation exposure. Once a patient is scanned, data is initially stored on the Philips software (IntelliSpace Portal). This portal was the source of data collection and contains the raw, uncompressed data which were then stored onto DVD-R discs in order to be imported into the visualization software.

2.3 | Data collection

CT images were imported into Avizo v9.0. (Visualization Sciences Group Inc) and 3D models of the vertebral columns were computed (Figure 1a,b). The cross-sectional areas of the right (RF) and left (LF) transverse foramina and the vertebral arteries passing through the right (RA) and left (LA) foramina were measured on the same individuals from C1 to C6. The best-fit plane to each foramen was identified by placing landmarks along the foraminal opening and using the option "Points to Fit" in the Avizo software (Figure 1c). A cross-section was then virtually extracted (Figure 1d,e). The cross-sectional areas of the transverse foramina (RF and LF) and of the vertebral arteries (RA and LA) were measured (mm^2) by semi-automatically segmenting the bony opening and the lumen of the arteries in Avizo using the module "Material statistics" (Figure 1f). This module computes statistical quantities (in this case cross-sectional areas) for the regions defined in the segmentation file (i.e., pixels attributed to the opening of the foramina). The voxel size is used to calculate the value.

2.4 | Statistical analyses

Normality tests (Shapiro Wilk's test) applied to the data set indicate that the distribution of RF, LF, RA, and LA are significantly different from the normal distribution. We thus log-transformed (base 10) our

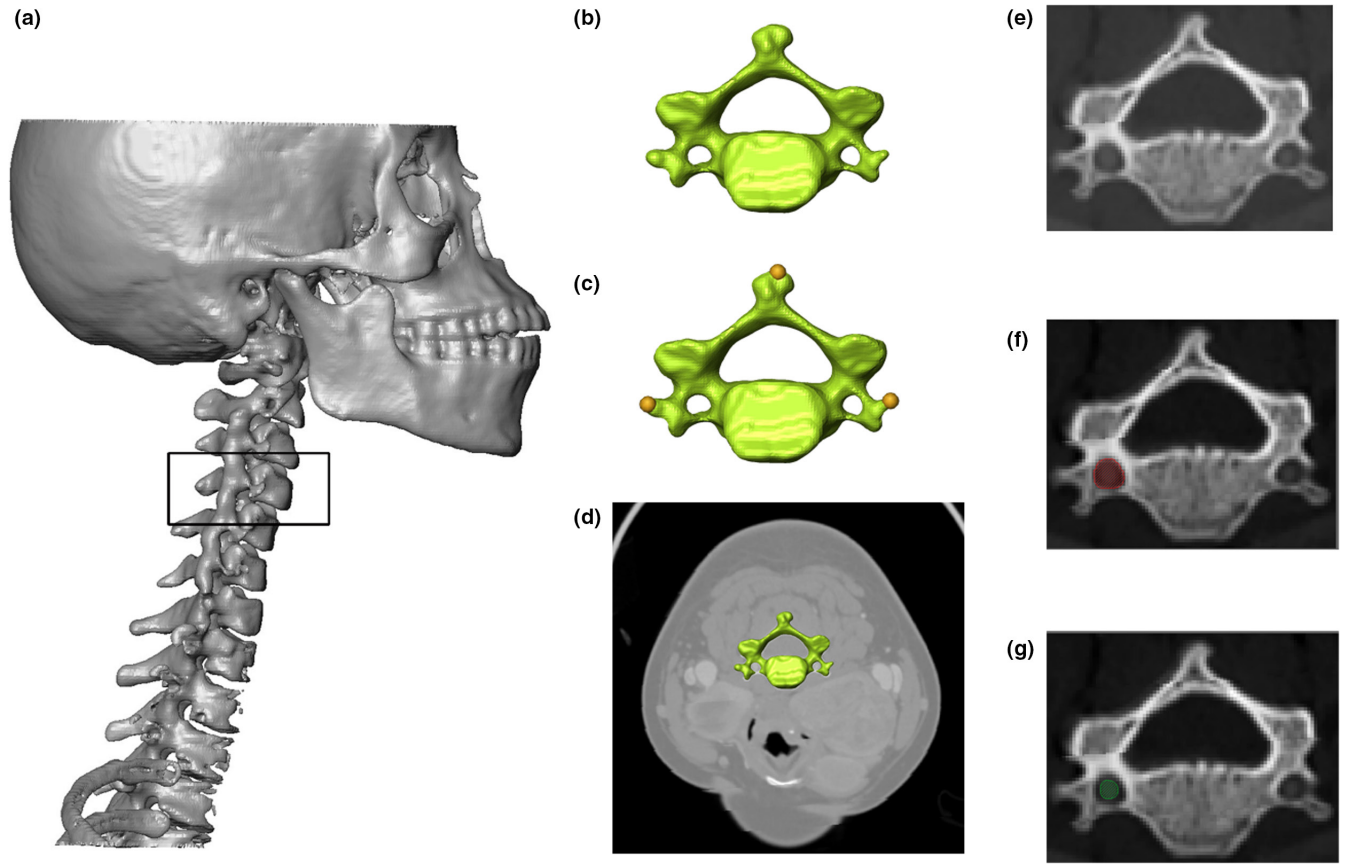

FIGURE 1 Measurement of the cross-sectional areas of the transverse foramina and vertebral arteries in the fourth cervical vertebra. 3D renderings of the cervical portion of the vertebral column (a) and the fourth cervical vertebrae (b). Position of the three landmarks (c) used to place the best-fit plane (d). Extraction of the cross-section (e) and segmentation of the transverse foramen of interest (f) and the corresponding vertebral artery (g)

data to remove the skewness of RF, LF, RA, and LA. The means of RF and LF and RA and LA were compared using a t-test. We tested the hypothesis of a significant correlation between RF and RA and between LF and LA using a Pearson correlation test. We then generated equations using a simple linear regression to predict the size of the arteries using the size of the transverse foramina as the predictor variable. Finally, to evaluate the performance of our model, we applied a leave-one-out cross-validation approach. All of the statistical analyses have been performed using RStudio (RStudio Team, 2015) and the packages "car" and "caret." For all of our tests, we consider that the results are statistically significant when the *p*-value is lower than 0.05. Each vertebra and each side were statistically investigated.

Intra- and inter-observer tests for measurement accuracy were run by two observers (E.J. and L.P.) who measured the vertebral arteries and foramina of the same individual. Differences recorded were less than 5%.

3 | RESULTS

Measurements of cross-sectional areas of RF and LF transverse foramina and the RA and LA are summarized in Table 1. The cross-sectional areas of RF and LF and RA and LA ranged between 13.40 and 71.25 mm^2 and between 4.53 and 29.40 mm^2, respectively. Overall, the cross-sectional areas of the arteries thus represent approximately 35% of the cross-sectional areas of the transverse foramina. RF and LF were larger in the atlas and axis as compared to the rest of the cervical vertebrae, and the cross-sectional areas increased from C3 to C6 (Table 1, Figure 2). On the contrary, RA and LA remained relatively constant (i.e., with a mean ranging from 10.60 to 12.82 mm^2) throughout the cervical segment of the vertebral column (Table 1, Figure 2).

The means of RF and LF, and RA and LA (Figure 3), did not significantly differ according to the results of the *t*-test. If we consider each side of the vertebrae separately and together, the transverse foramina and corresponding arteries are significantly correlated for C2, C3, C4, C5, and C6 with a correlation coefficient ranging from 0.54 to 0.87 (Table 2). The strongest correlation (0.87) is reported for the right side of C6.

Using linear regression, we computed the coefficients (i.e., intercepts and slopes) to generate a model formula for our three categories of vertebrae (Table 2). Because our study did not detect significant asymmetry in the cross-sectional areas, we also consider the formulas combining both sides (but the coefficients for each side

TABLE 1 Cross-sectional areas of the right (RF) and left (LF) transverse foramina and of the right (RA) and left (LA) vertebral arteries (mm^2). C: cervical vertebra

Vertebra	RF	LF	RA	LA
C1				
Mean	38.34	39.33	10.69	10.90
Range	22.78–58.24	24.62–51.34	7.11–16.97	5.19–16.19
C2				
Mean	37.64	38.39	11.35	12.82
Range	22.83–61.80	26.07–57.10	4.92–19.59	7.95–21.31
C3				
Mean	27.83	27.70	11.61	10.59
Range	17.67–50.48	15.47–36.79	5.18–29.40	7.03–16.09
C4				
Mean	25.91	26.84	10.74	10.60
Range	17.55–37.70	13.40–44.03	4.53–27.19	4.62–19.78
C5				
Mean	30.61	30.14	10.93	12.06
Range	17.0–52.99	18.04–62.71	5.01–21.73	6.84–26.44
C6				
Mean	30.69	32.02	10.92	12.39
Range	14.31–71.25	14.62–58.16	5.57–24.01	6.22–22.93
Mean	31.83	32.24	11.04	11.56
Range	14.31–71.25	13.40–62.71	4.53–29.40	4.62–26.44

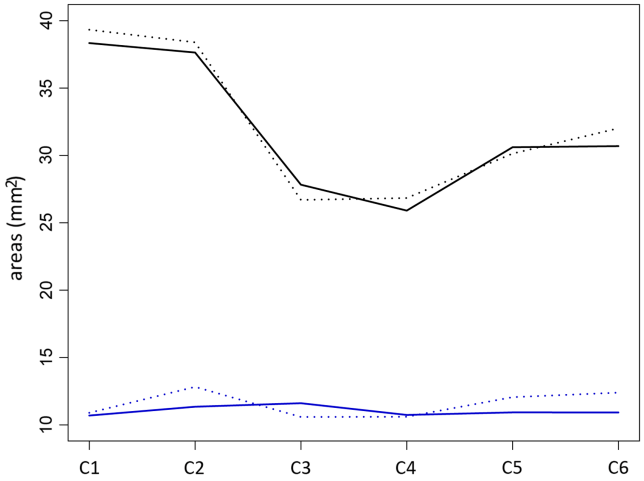

FIGURE 2 Variation of the cross-sectional areas of the right (solid lines) and left (dashed lines) foramina (dark lines) and arteries (blue lines) across the cervical (C) vertebrae

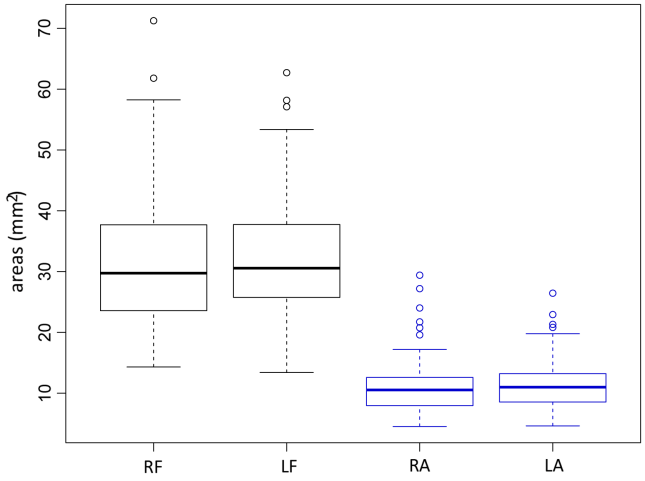

FIGURE 3 Boxplots of the cross-sectional areas of the right (RF) and left (LF) foramina (dark) and of the right (RA) and left (LA) arteries (blue). Each boxplot presents the data minimum (i.e., lowest horizontal bar), the first quartile (i.e., the lower edge of the box), median (i.e., bar inside the box), third quartile (i.e., the upper edge of the box), and data maximum (i.e., highest bar)

are given in Table 2). For instance, when using data from the right side of C2 the equation is $\log(x) = 1.098*\log(y)-0.6844$, in which x is the cross-sectional area of the artery and y the transverse foramen, while for the left side the equation is $\log(x) = 1.0081*\log(y)-0.4974$. When the two sides are combined, the equation is then $\log(x) = 0.8718*\log(y)-0.3$.

We applied a leave-one-out cross-validation approach to the data set that contains value measurements from the two sides separately and together (Table S1). The root mean squared error (RMSE) is particularly low for C2, C3, and C6, higher for C4 and C5, and particularly high for C1 left side (for which the correlation between the cross-sectional areas of the foramen and artery is not significant, see Table 2). We observe a similar trend with the mean absolute error (MAE), C1 left side standing out as being particularly high (Table S1). R^2 is particularly high for C2, C3, C4, C5, and C6, but much lower for

TABLE 2 Pearson correlation coefficient (*r*) and coefficients (intercept and slope) computed by applying a linear regression model to the cross-sectional areas of the cervical (C) vertebrae. Each vertebra and each side are considered independently. The coefficients for each vertebra when considering the mean values of both sides are also provided

Vertebra	Side	*r*	Intercept	Slope
C1	Right	0.38	0.4104	0.3854
	Left	0.41	−0.1194	0.7142
	Both sides	0.23	0.5013	0.3236
C2	Right	0.79[a]	−0.6844	1.0980
	Left	0.71[a]	−0.4974	1.0081
	Both sides	0.70[a]	−0.3000	0.8718
C3	Right	0.84[a]	−0.9536	1.3821
	Left	0.63[a]	−0.1055	0.7875
	Both sides	0.82[a]	−0.6116	1.1476
C4	Right	0.75[a]	−0.9864	1.4089
	Left	0.54[a]	0.03023	0.68746
	Both sides	0.62[a]	−0.3260	0.9421
C5	Right	0.77[a]	−0.3068	0.9003
	Left	0.76[a]	−0.3344	0.9496
	Both sides	0.75[a]	−0.2759	0.8932
C6	Right	0.87[a]	−0.2118	0.8384
	Left	0.80[a]	−0.2544	0.8898
	Both sides	0.83[a]	−0.1075	0.7823

[a]Significant correlation coefficients.

C1 (Table S1). Altogether, these parameters indicate that our models for C2, C3, C4, C5, and C6 are more accurate and have a higher predictive value than the model built on data obtained for C1.

4 | DISCUSSION

Our study provides preliminary data on the spatial relationship between the transverse foramina and the size of the arteries within extant human cervical vertebrae. As in the study by Cagnie et al. (2005), we did find that the size of the foramina increased from C3 to C6, which is also confirmed, to a lesser extent, by Malla et al. (2018). However, contrary to previous studies (Sanelli et al., 2002; Cagnie et al., 2005; Kim et al., 2012; Kotil & Kilincer, 2014; Abd El Gawad et al., 2019; but see Sangari et al., 2015 about the size of the foramina), our analysis did not show any significant asymmetries between right and left transverse foramina or arteries. Such discrepancies could be related to differences in protocols (e.g., diameters measured in previous studies versus cross-sectional areas in the present study, non-homologous cross-sections) or to the relatively small cohort of the present study. However, measurements of the mean cross-sectional areas of the transverse foramina reported by Alicioglu et al. (2015) for C1-C6 and of Sanchis-Gimeno et al. (2018) for C6 fall within the range of values described in this study (Table 1). Sanelli et al. (2002) investigated the percent area of the transverse foramen occupied by the vertebral artery and found level-to-level variability in the areas of the transverse foramina with a variance of 24.23 that impacted their assessment of the percent area occupied by the arteries (variance of 36.79). Their results support our approach of generating different equations depending on the position of the vertebrae considered. Additionally, we found that the arteries occupy 35% of the foramen areas (mean computed using the measurements for C1-C2), which is close to the estimation from Sanelli et al. (2002) (i.e., 33.9%) but lower than the estimation provided by Boyer and Harrington (2019) for *Homo sapiens* (63%). Within the limit of our sample, our analysis documents a statistically significant correlation between the cross-sectional areas of the transverse foramina and vertebral arteries from C2 to C6, which is further supported by the results from Kim et al. (2012). The lack of correlation in C1 might be explained by the specific geometry of this vertebra and its pivotal role in the biomechanics of the neck (Nalley & Grider-Potter, 2017). Similarly, Kotil and Kilincer (2014) noted a strong correlation between the diameters of the transverse foramina and blood volume in C6, reinforcing the potential of dry bones for estimating blood flow.

Given that we investigated the complete cervical segment through which the vertebral arteries flow, measurements of fossil vertebral remains from any positions between C2 to C6 that preserve the transverse foramina may be directly compared to our database. Because our study is restricted to extant humans, at this stage we recommend that our equations are applied to fossil humans only. While the size of the vertebral arteries does not substantially vary across the cervical vertebrae, we noticed important variations in the size of the foramina. More particularly, the foramina in the atlas and axis are particularly large as compared to the other vertebrae and to the actual size of the arteries, which may explain the relatively weak correlation in C1. However, given that atlas and axis are frequently recovered from the fossil hominin record (e.g., Lovejoy et al., 1982; Gómez-Olivencia et al., 2007; Beaudet et al., 2020), investigating the predictive power of such structures was essential. We do acknowledge that uncertainties remain whether the human reference is the most appropriate model for reconstructing fossil hominin soft tissues. Nonetheless, within the limits of our sample, our study introduces an essential comparative database for a better understanding of the evolutionary story of cervical arteries in the fossil record.

ACKNOWLEDGMENT

This research has been funded by the National Research Foundation of South Africa (Research Development Grants for Y-Rated Researchers, grant number 129336) and the South Africa/France (PROTEA) Joint Research Programme (grant number 129923) as well as the Bakeng se Afrika project co-funded by the Erasmus plus programme (597924-EPP-1-2018-1-ZA-EPPKA2-CBHE-JP 2018-3229). Ethical clearance (49/2020,IR) for the use of CT scans was obtained from the Research Ethics committee of the relevant tertiary institution (NHREC No: REC210408-003).

AUTHOR CONTRIBUTIONS

Designed/performed research: A.B., E.d.J., L.P., N.A., A.O.; collected samples: N.A.; collected data: E.d.J., L.P.; analyzed/interpreted data: A.B., E.d.J., L.P. wrote/revised the paper: A.B., E.d.J., L.P., N.A., A.O.

DATA AVAILABILITY STATEMENT

CT scans cannot be made publicly available as sharing these data requires ethical clearance from the Research Ethics committee.

ORCID

Edwin de Jager https://orcid.org/0000-0003-3199-8566
Lané Prigge https://orcid.org/0000-0002-8168-9238
Anna Oettlé https://orcid.org/0000-0002-5665-6581
Amélie Beaudet https://orcid.org/0000-0002-9363-5966

REFERENCES

Abd El Gawad, F.A., Shaaban, M.H., Shuaib, D.M. & Shallan, H.M. (2019) Anatomical variations of the vertebral artery and its relation to the atlas vertebra – radiological and dry bone study. *European Journal of Anatomy*, 23(1), 49–58.

Alicioglu, B., Gulekon, N. & Akpinar, S. (2015) Age-related morphologic changes of the vertebral artery in the transverse process. Analysis by multidetector computed tomography angiography. *The Spine Journal*, 15, 1981–1987.

Beaudet, A., Clarke, R.J., Heaton, J.L., Pickering, T.R., Carlson, K.J., Crompton, R. et al. (2020) The atlas of StW 573 and the late emergence of human-like head mobility and brain metabolism. *Scientific Reports*, 10, 4285.

Boyer, D.M. & Harrington, A.R. (2018) Scaling of bony canals for encephalic vessels in euarchontans: Implications for the role of the vertebral artery and brain metabolism. *Journal of Human Evolution*, 114, 85–101.

Boyer, D.M. & Harrington, A.R. (2019) New estimates of blood flow rates in the vertebral artery of euarchontans and their implications for encephalic blood flow scaling: a response to Seymour and Snelling (2018). *Journal of Human Evolution*, 128, 93–98.

Cagnie, B., Barbaix, E., Vinck, E., D'Herde, K. & Cambier, D. (2005) Extrinsic risk factors for compromised blood flow in the vertebral artery: anatomical observations of the transverse foramina from C3 to C7. *Surgical and Radiologic Anatomy*, 27(4), 312–316.

Gómez-Olivencia, A., Carretero, J.M., Arsuaga, J.L., Rodríguez-García, L., García-González, R. & Martínez, I. (2007) Metric and morphological study of the upper cervical spine from the Sima de los Huesos site (Sierra de Atapuerca, Burgos, Spain). *Journal of Human Evolution*, 53(1), 6–25.

Hublin, J.-J., Neubauer, S. & Gunz, P. (2015) Brain ontogeny and life history in Pleistocene hominins. *Philosophical Transactions of the Royal Society B: Biological Sciences*, 370(1663), 20140062.

Kim, C., Lee, S.-H., Park, S.S., Kim, B.J., Ryu, W.-S., Kim, C.K. et al. (2012) A quantitative comparison of the vertebral artery and transverse foramen using CT angiography. *Journal of Clinical Neurology*, 8(4), 259–264.

Kotil, K. & Kilincer, C. (2014) Sizes of the transverse foramina correlate with blood flow and dominance of vertebral arteries. *The Spine Journal*, 14, 933–937.

Leonard, W.R. & Robertson, M.L. (1994) Evolutionary perspectives on human nutrition: The influence of brain and body size on diet and metabolism. *American Journal of Human Biology*, 6(1), 77–88.

Leonard, W.R., Robertson, M.L., Snodgrass, J.J. & Kuzawa, C.W. (2003) Metabolic correlates of hominid brain evolution. *Comparative Biochemistry and Physiology – part A: Molecular & Integrative Physiology*, 136(1), 5–15.

Lieberman, D.E. (2011) *The evolution of the human head*. Cambridge: Harvard University Press.

Lovejoy, C.O., Johanson, D.C. & Coppens, Y. (1982) Elements of the axial skeleton recovered from the Hadar formation: 1974-1977 collections. *American Journal of Physical Anthropology*, 57, 631–635.

Malla, H.P., Kim, S.B., Won, J.S. & Choi, M.K. (2018) Study of the transverse foramen in the subaxial cervical spine in Korean patients with degenerative changes: an anatomical note. *Neurospine*, 15(2), 163–168. https://doi.org/10.14245/ns.1836004.022

Moore, K.L., Agur, A.M.R. & Dalley, A.F. (2018) *Clinically oriented anatomy*, 8th edition. Baltimore: Wolters Kluwer.

Nalley, T.K. & Grider-Potter, N. (2017) Functional analyses of the primate upper cervical vertebral column. *Journal of Human Evolution*, 107, 19–35.

RStudio Team. (2015) *RStudio: Integrated Development for R*. Boston, MA: RStudio, Inc. http://www.rstudio.com/

Sanchis-Gimeno, J.A., Blanco-Perez, E., Llido, S., Perez-Bermejo, M., Nalla, S. & Mata-Escolano, F. (2018) Can the transverse foramen/vertebral artery ratio of double transverse foramen subjects be a risk for vertebrobasilar transient ischemic attacks? *Journal of Anatomy*, 233, 341–346.

Sanelli, P.C., Tong, S., Gonzalez, R.G. & Eskey, C.J. (2002) Normal variation of vertebral artery on CT angiography and its implications for diagnosis of acquired pathology. *Journal of Computer Assisted Tomography*, 26, 462–470.

Sangari, S.K., Dossous, P.M., Heineman, T. & Mtui, E.P. (2015) Dimensions and anatomical variants of the foramen transversarium of typical cervical vertebrae. *Anatomy Research International*, 391823.

Seymour, R.S., Bosiocic, V. & Snelling, E.P. (2016) Fossil skulls reveal that blood flow rate to the brain increased faster than brain volume during human evolution. *Royal Society Open Science*, 3, 160305.

Standring, S., Borley, N.R. & Gray, H. (2008) In: Standring, S. (Ed.) *Gray's anatomy: the anatomical basis of clinical practice*, 40th edition. Edinburgh: Churchill Livingstone/Elsevier.

SUPPORTING INFORMATION

Additional supporting information may be found in the online version of the article at the publisher's website.

How to cite this article: de Jager, E., Prigge, L., Amod, N., Oettlé, A. & Beaudet, A. (2022) Exploring the relationship between soft and hard tissues: The example of vertebral arteries and transverse foramina. *Journal of Anatomy*, 241, 447–452. Available from: https://doi.org/10.1111/joa.13681